Electronic Supplementary Information

Structural phase transition and dielectric response in two novel cyano-bridged coordination polymers synthesized by sealing the incomplete cyano-bridged cage

Zhuoer Cai,‡[a] Xiu-Ni Hua,‡*[b] Yinan Zhang,[a] Jian Chen,[a] Kai Sun,[c] Zining Wang,[a] Xianmin Liu,[a] Xinyi Zhang,[a] Shiyue Xiao[a] and Baiwang Sun[a]

[a.] *School of Chemistry and Chemical Engineering, Southeast University, Nanjing 211189, P. R. China.*

[b.] *School of Environmental Science, Nanjing Xiaozhuang University, Nanjing 211171, P. R. China. E-mail address: huaxiuni@njxzc.edu.cn*

[c.] *Jiangsu Key Laboratory for Biomass-based Energy and Enzyme Technology, School of Chemistry and Chemical Engineering, Huaiyin Normal University, Huaian 223300, China* ◦

Contents:

Calculations of Molecular structure

Molecular electrostatic potential surfaces are important space function in quantum chemistry. It can be used to explain and predict electrostatic interactions between molecules, electrostatic potential charge fitting for molecular simulation, nucleophilic and electrophilic reaction sites. Molecular electrostatic potential surfaces and molecular frontier orbital energy of *N,N,N′,N′*-tetramethylethylenediamine were calculated by Gaussian 16 package with DFT/B3LYP and 6-311^{++}g (d,p) basis sets after optimization (Fig. S5, Fig. S6 and Fig. S7). The molecular electrostatic potential surfaces were drawn on the electron density isosurface of 0.004 Bohr Å^{-3}. The maximum and minimum value of electrostatic potential are 0.27 and 0.35 eV. The electrostatic potential involved in the analyses was evaluated by Multiwfn and VMD based on the highly effective algorithm.[1,2] The spatial configuration of organic gust cation of calculation result is consistent with it in single crystal structure.

The Hirshfeld Surface was analyzed and produced on the basis of its single crystal data using CrystalExplorer v17.0 software (Fig. S8, Fig. S9, Fig. S10, Fig. S11 and Fig. S12,). Pairs of d_i and d_e values were used to depict the 2D fingerprint plots.[3] It can be seen from Fig. S9 and Fig. S10, at 323 K, organic cation became server disorder over two sites. The interactions between molecules also changed, especially H···O interactions. For **2**, H···O interactions comprise 3.7 % of all interactions at 150 K, while H···O interactions comprise only 0.3 % of all interactions at 323 K. We surmise that the disorder movement of organic cations caused displacement of cyano-group skeleton and water molecules, inducing larger voids in the framework and less binding on water molecules. Thus, **1** and **2** are not stable enough and started to dehydration and form **3** and **4**.

SEM Measurement

SEM measurement was carried on a Navo nano SEM450. To enhance the electrical conductivity of the sample, platinum is sprayed on the surface of the sample. To fully reveal the morphology of the crystal, both smooth and rough areas of the crystal surface were photographed. It is obvious that there are more cracks on the surface of **3** and **4** than **1** and **2**, which were probably caused by the escape of water molecules. Water molecules in the center of the crystal were steamed out and cause a damage to the peripheral morphology of the crystal.

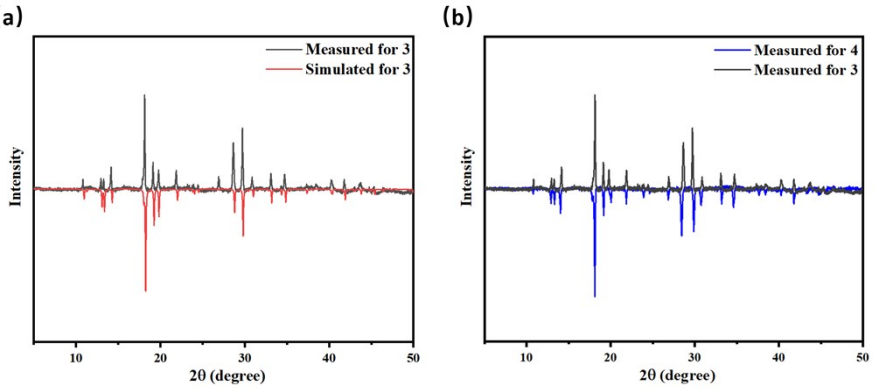

Fig. S1 PXRD patterns of **3** at room temperature and a simulated PXRD patterns (**a**). at room temperature. A comparison of PXRD patterns for **3** and **4** at room temperature (**b**).

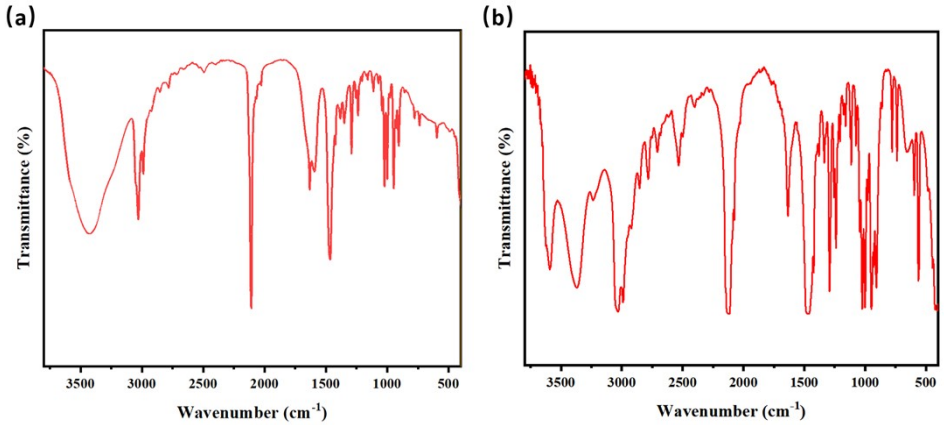

Fig. S2 Infrared spectrum of **3** and **4** at room temperature.

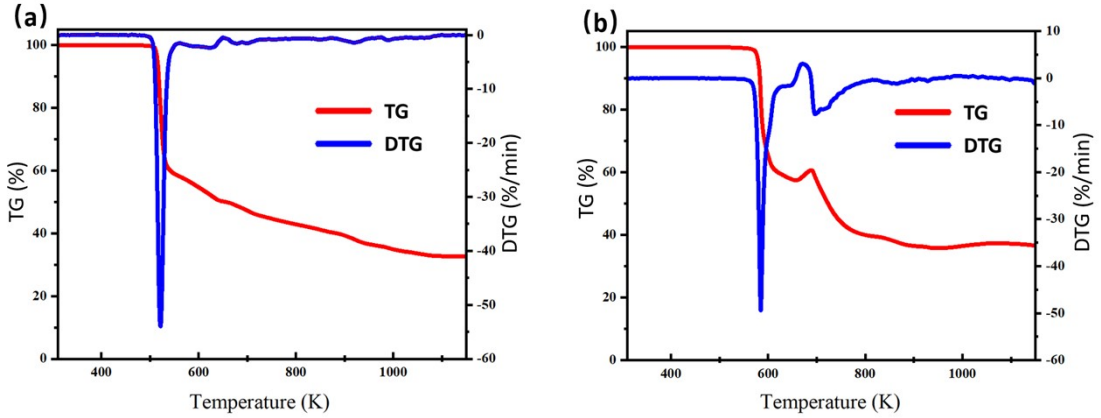

Fig. S3 TG result of **3** (**a**) and **4** (**b**).

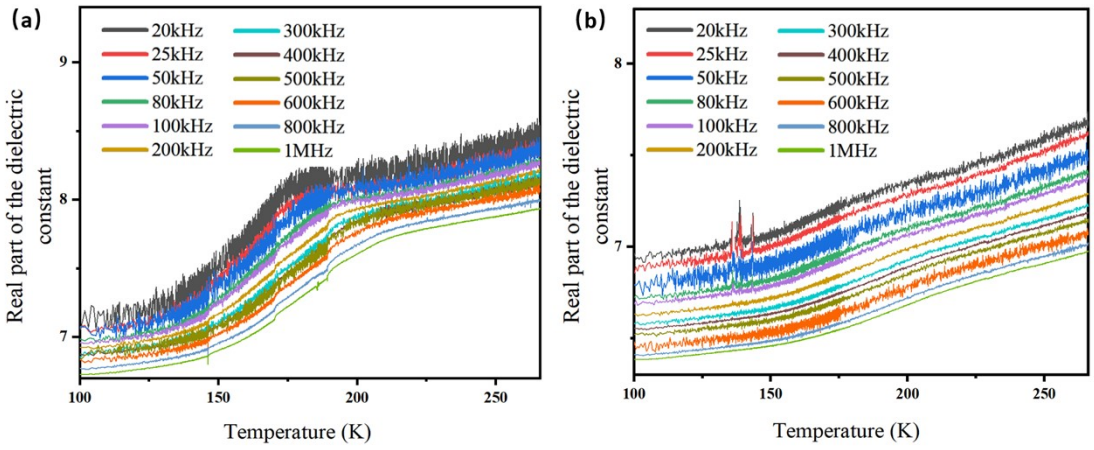

Fig. S4 Temperature dependence of the dielectric constant of **3** (**a**) and **4** (**b**) with different frequencies.

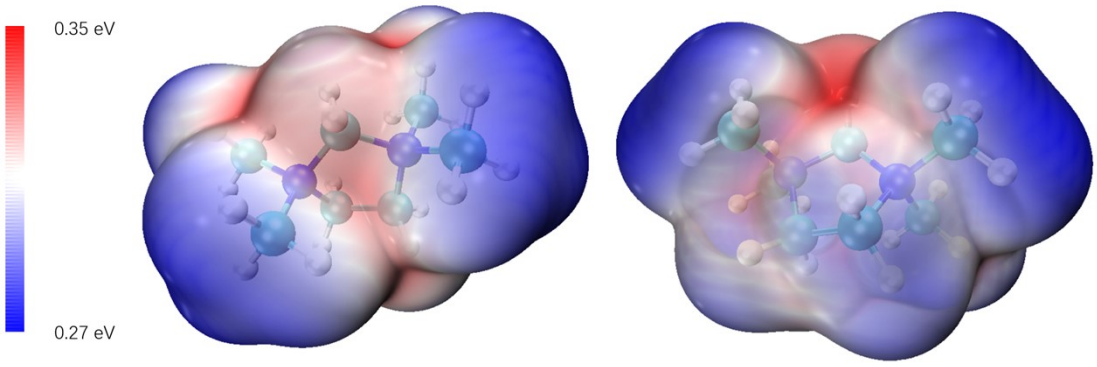

Fig. S5 Molecular Electrostatic potential surfaces of *N*,*N*,*N*′,*N*′-tetramethylethylenediamine.

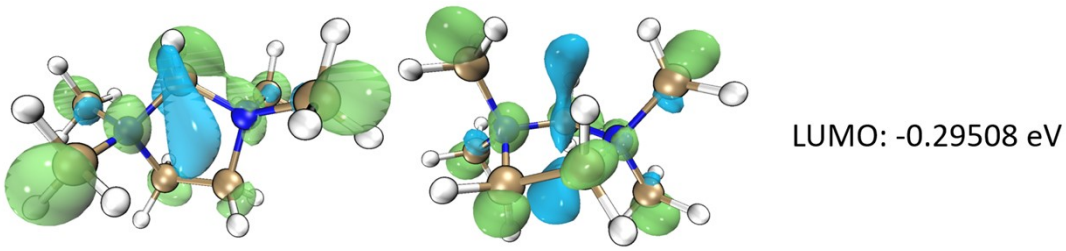

Fig. S6 Lowest Unoccupied Molecular Orbital of *N*,*N*,*N*′,*N*′-tetramethylethylenediamine.

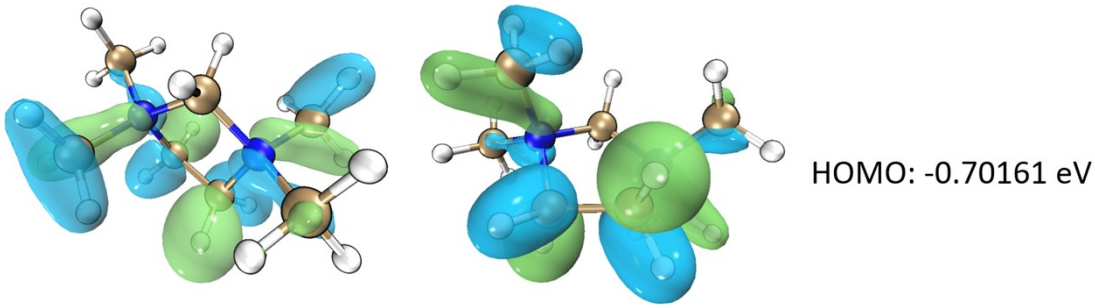

Fig. S7 Highest Occupied Molecular Orbital of *N*,*N*,*N*′,*N*′-tetramethylethylenediamine.

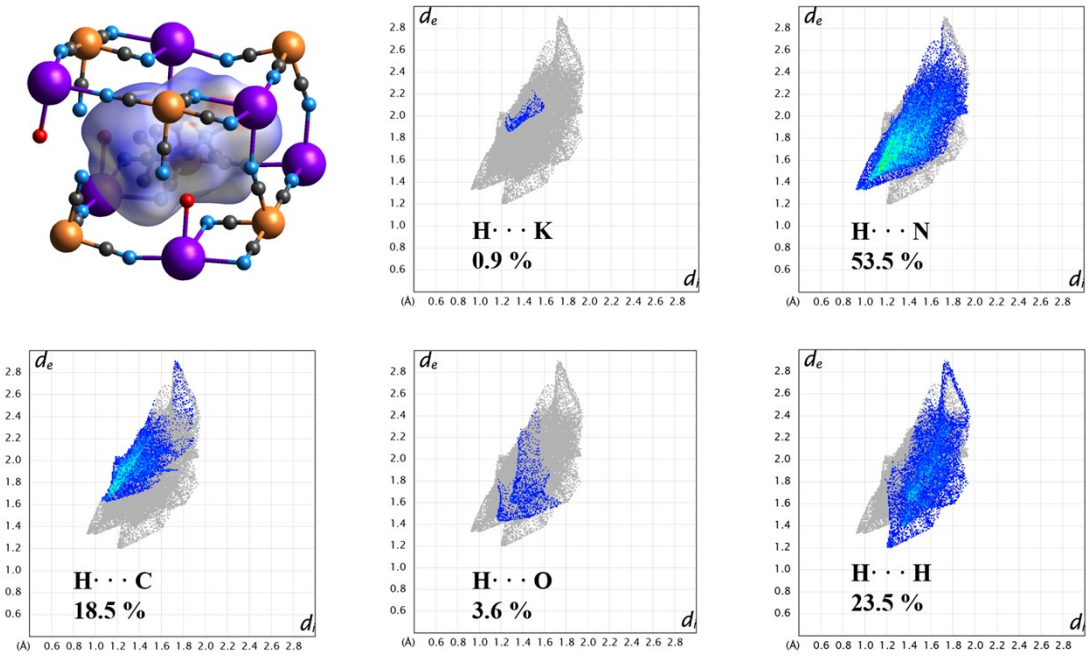

Fig. S8 3D d_{norm} Hirshfeld surface and 2D fingerprint plots of **1** at 150 K; the full fingerprint appears beneath each decomposed plot as a grey shadow.

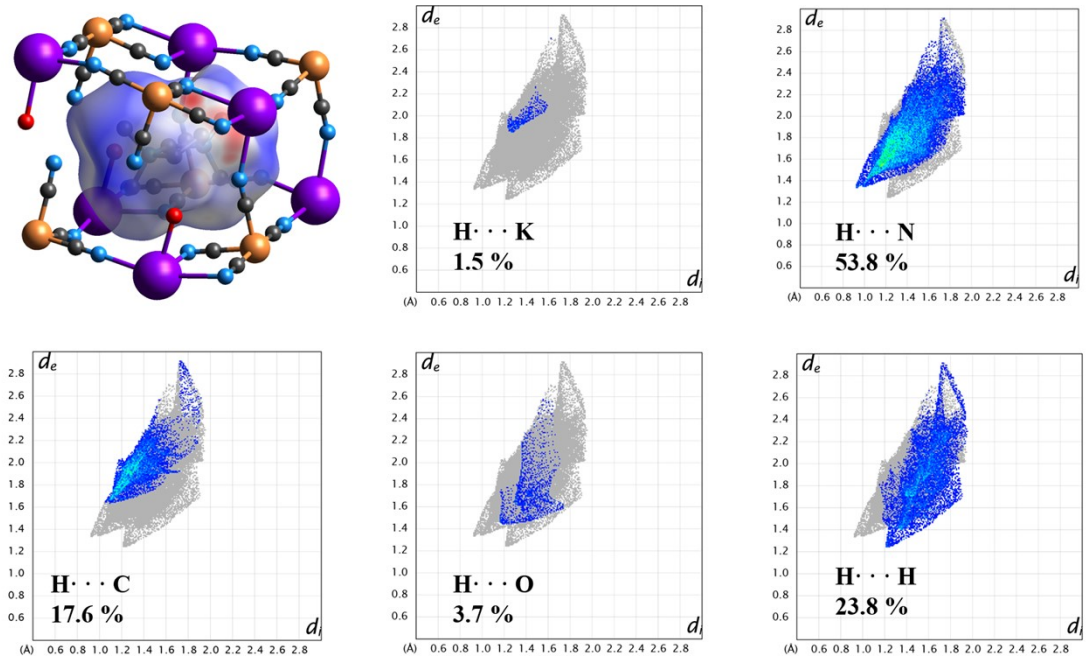

Fig. S9 3D d_{norm} Hirshfeld surface and 2D fingerprint plots of **2** at 150 K; the full fingerprint appears beneath each decomposed plot as a grey shadow.

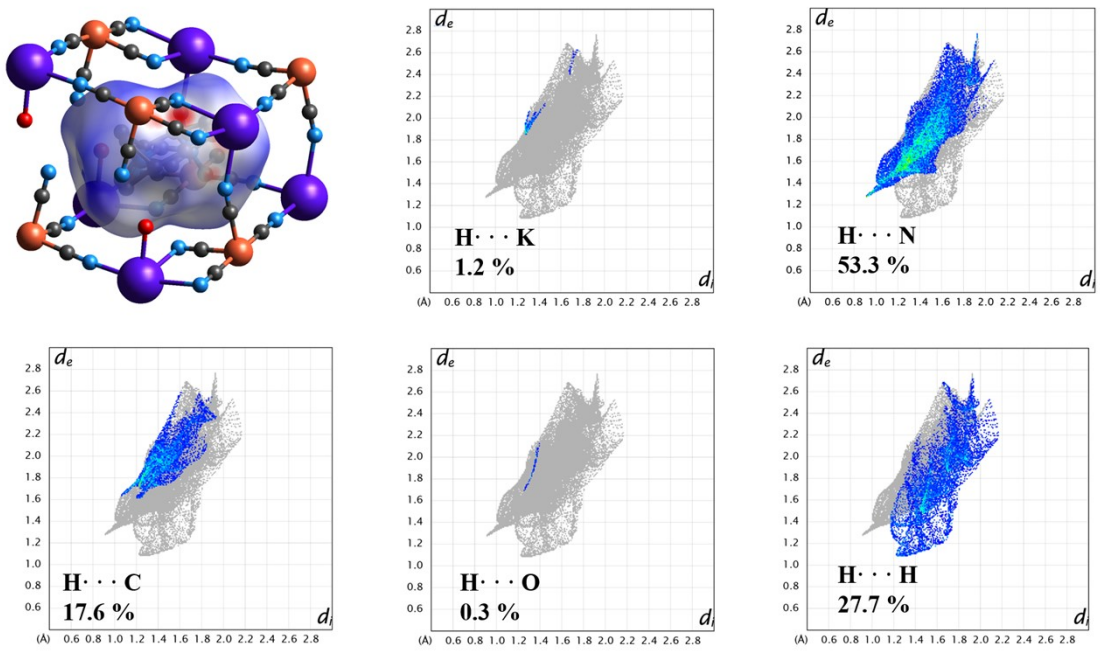

Fig. S10 3D d_{norm} Hirshfeld surface and 2D fingerprint plots of **2** at 323 K; the full fingerprint appears beneath each decomposed plot as a grey shadow.

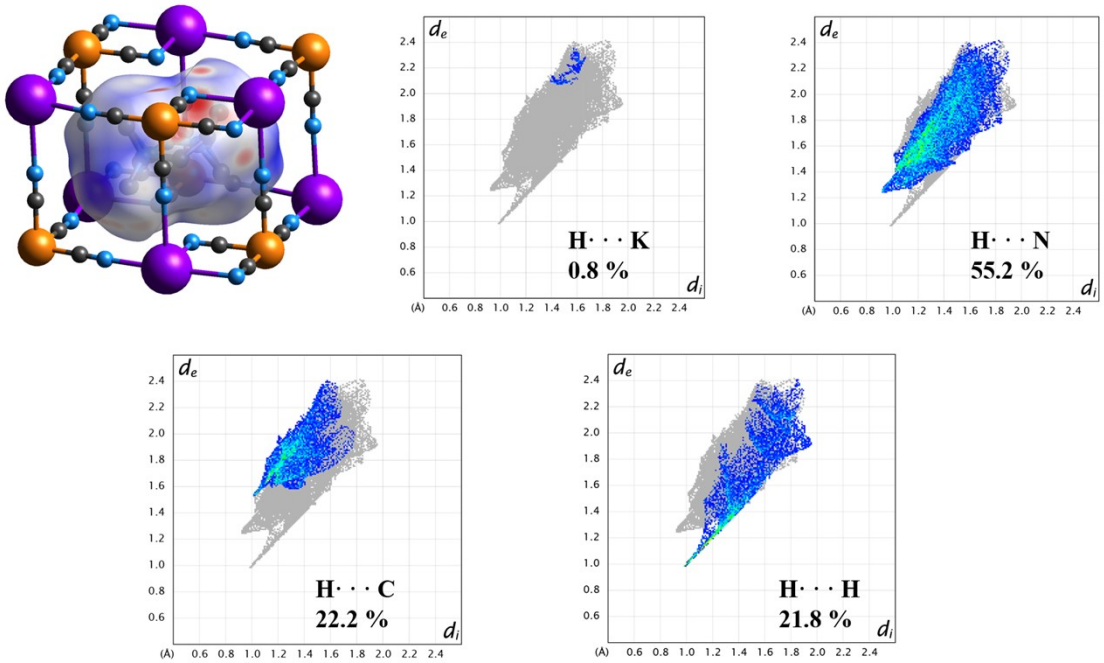

Fig. S11 3D d_{norm} Hirshfeld surface and 2D fingerprint plots of **3** at 100 K; the full fingerprint appears beneath each decomposed plot as a grey shadow.

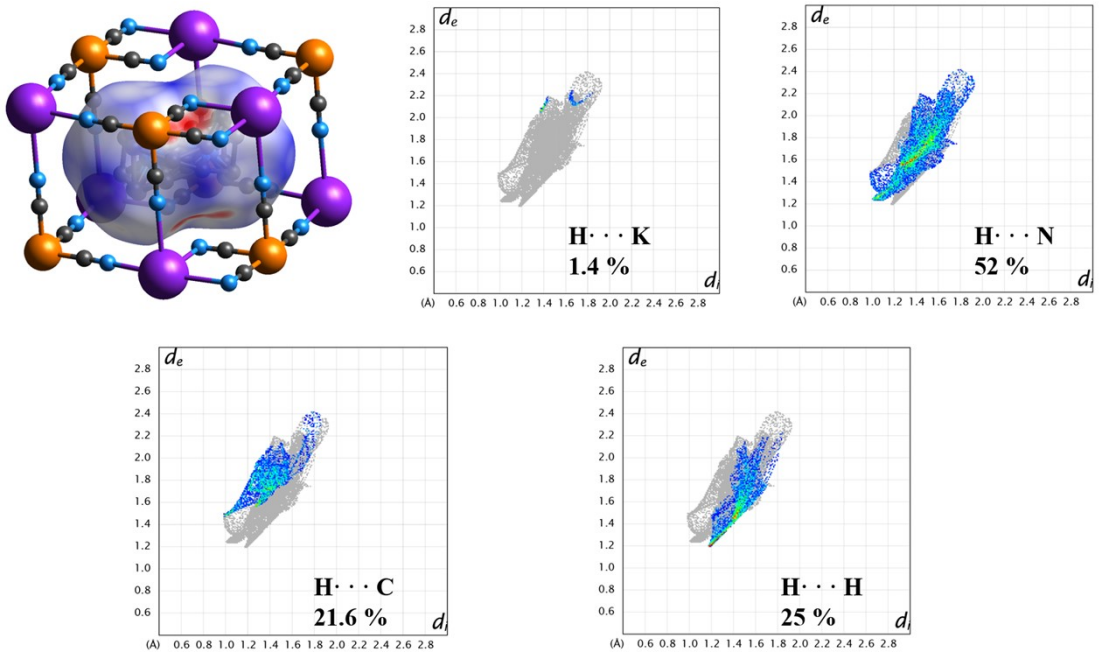

Fig. S12 3D d_{norm} Hirshfeld surface and 2D fingerprint plots of **3** at 323 K; the full fingerprint appears beneath each decomposed plot as a grey shadow.

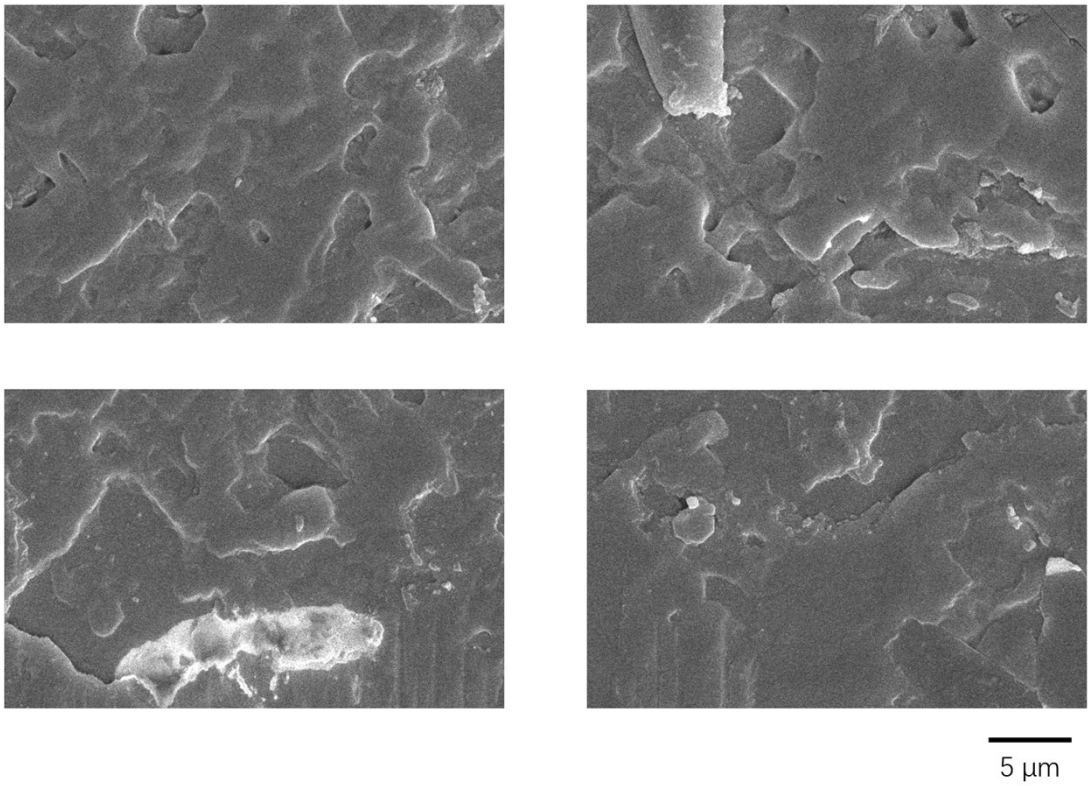

Fig. S13 SEM image of smooth area of **1** at room temperature.

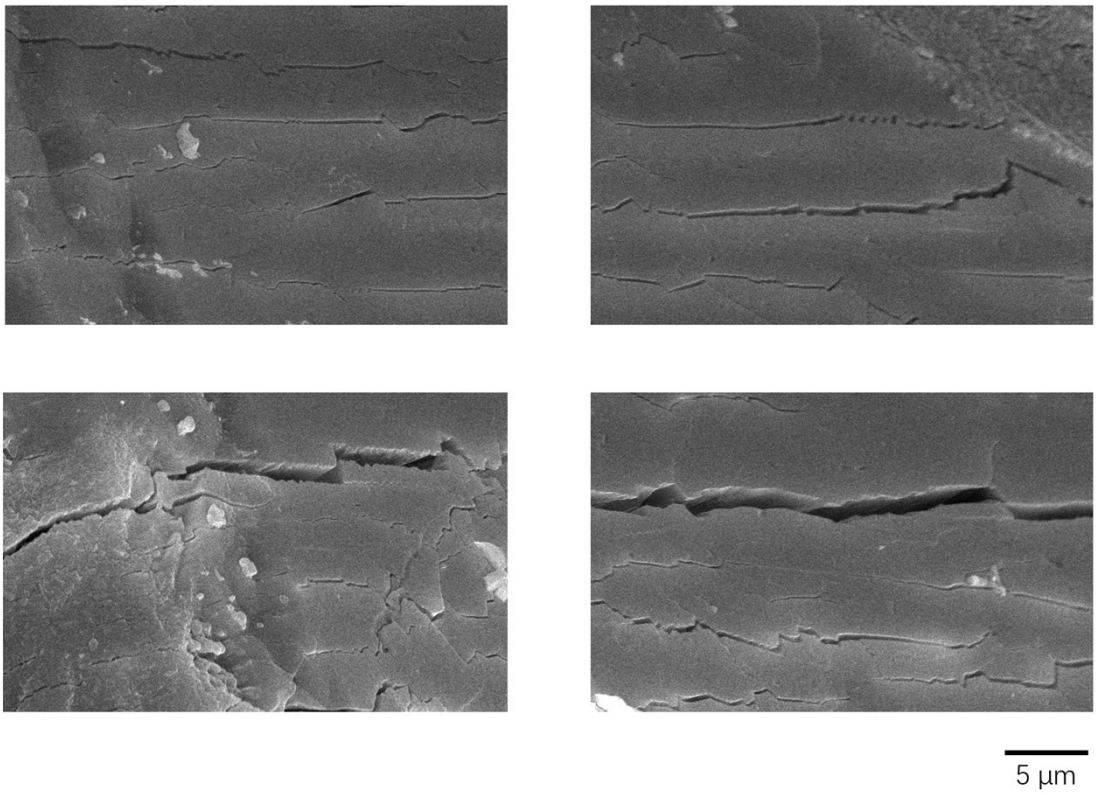

Fig. S14 SEM image of coarse area of **1** at room temperature.

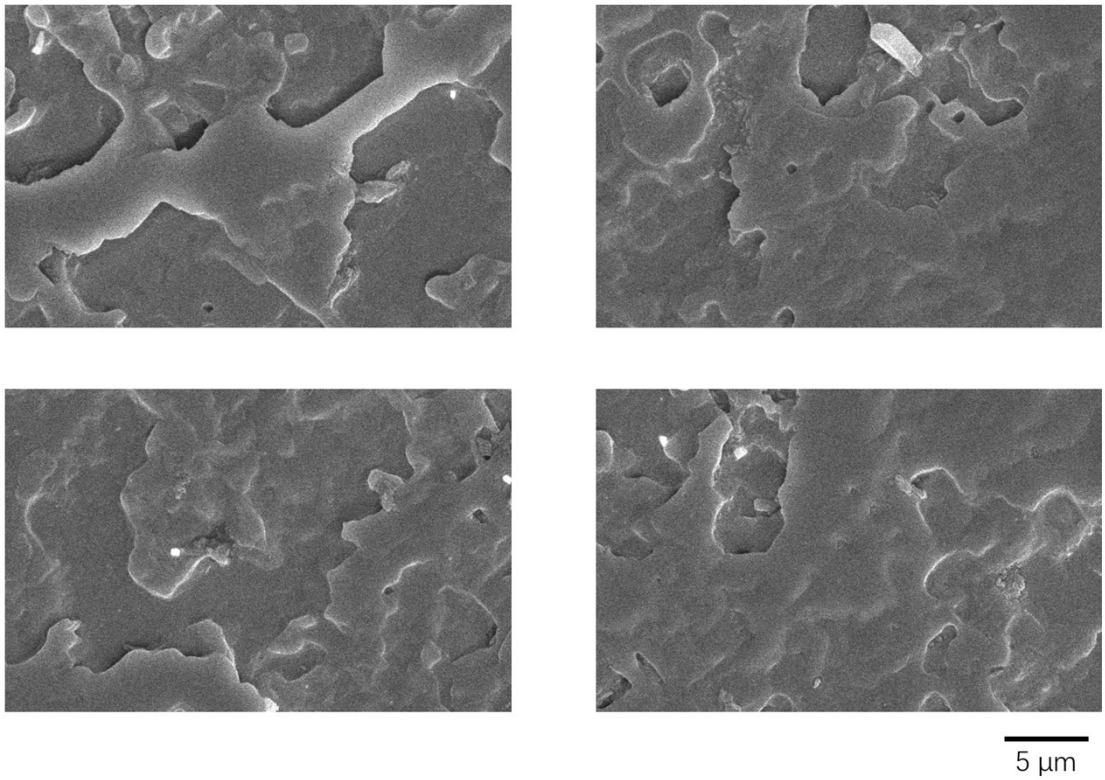

Fig. S15 SEM image of smooth area of **2** at room temperature.

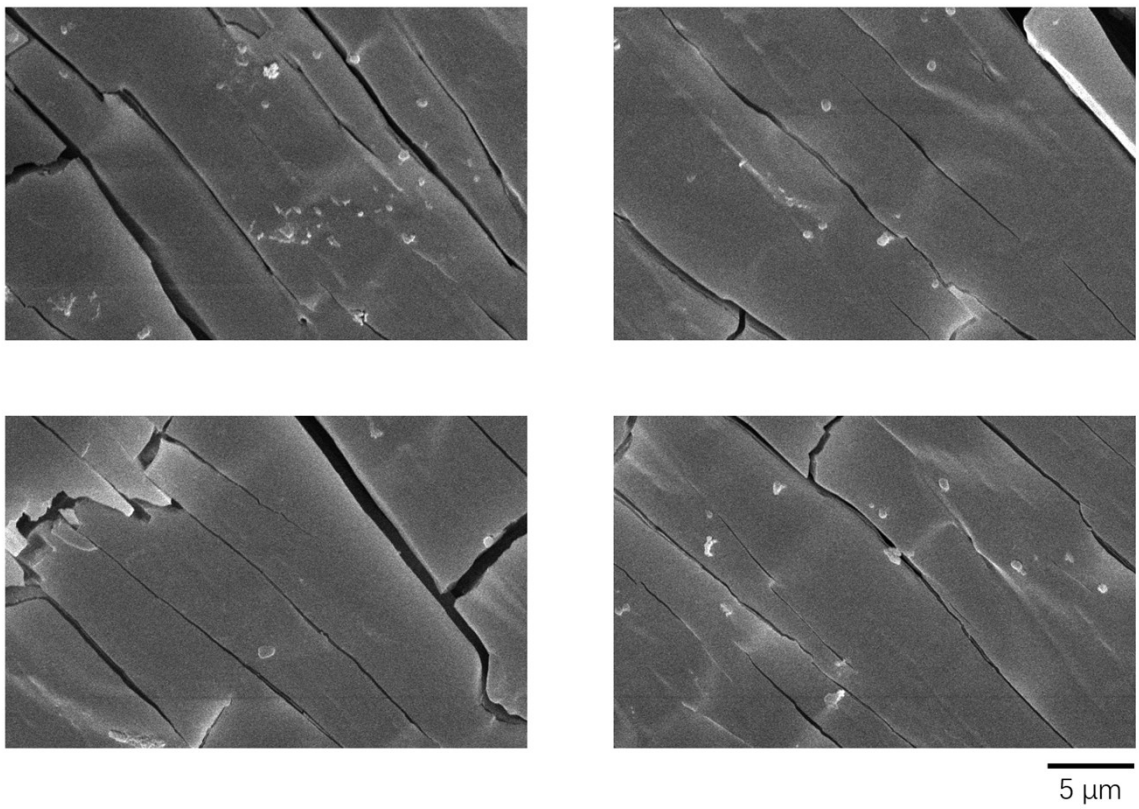

Fig. S16 SEM image of coarse area of **2** at room temperature.

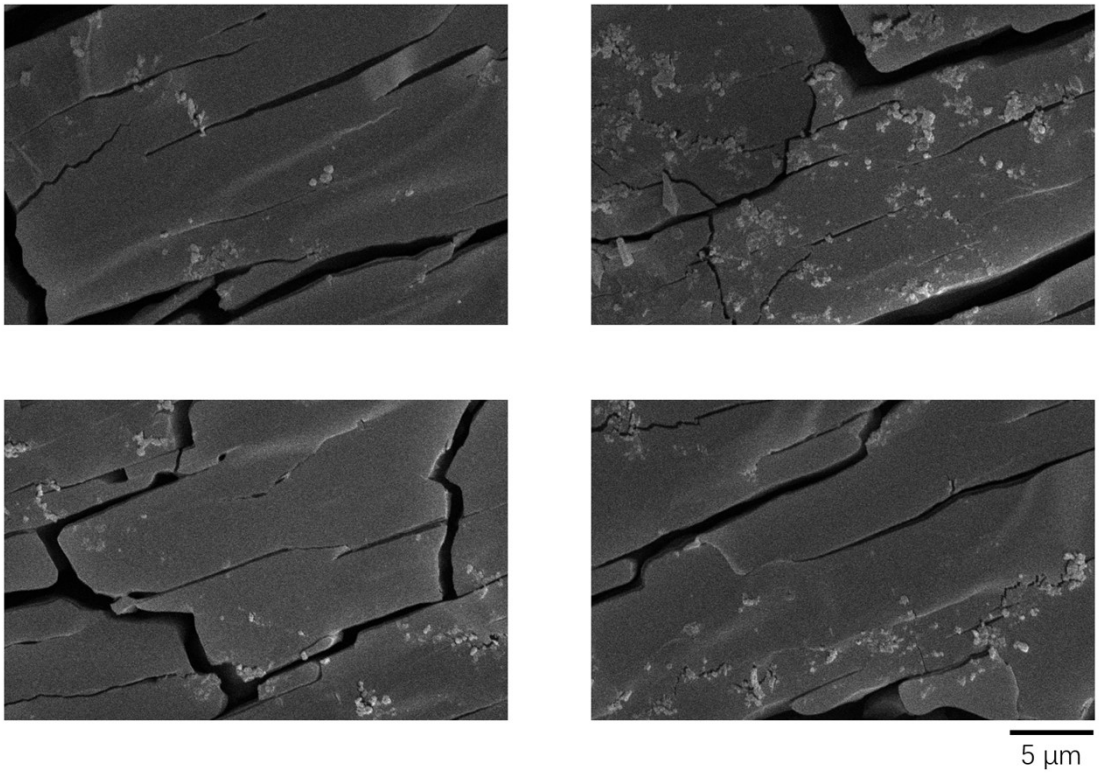

Fig. S17 SEM image of smooth area of **3** at room temperature.

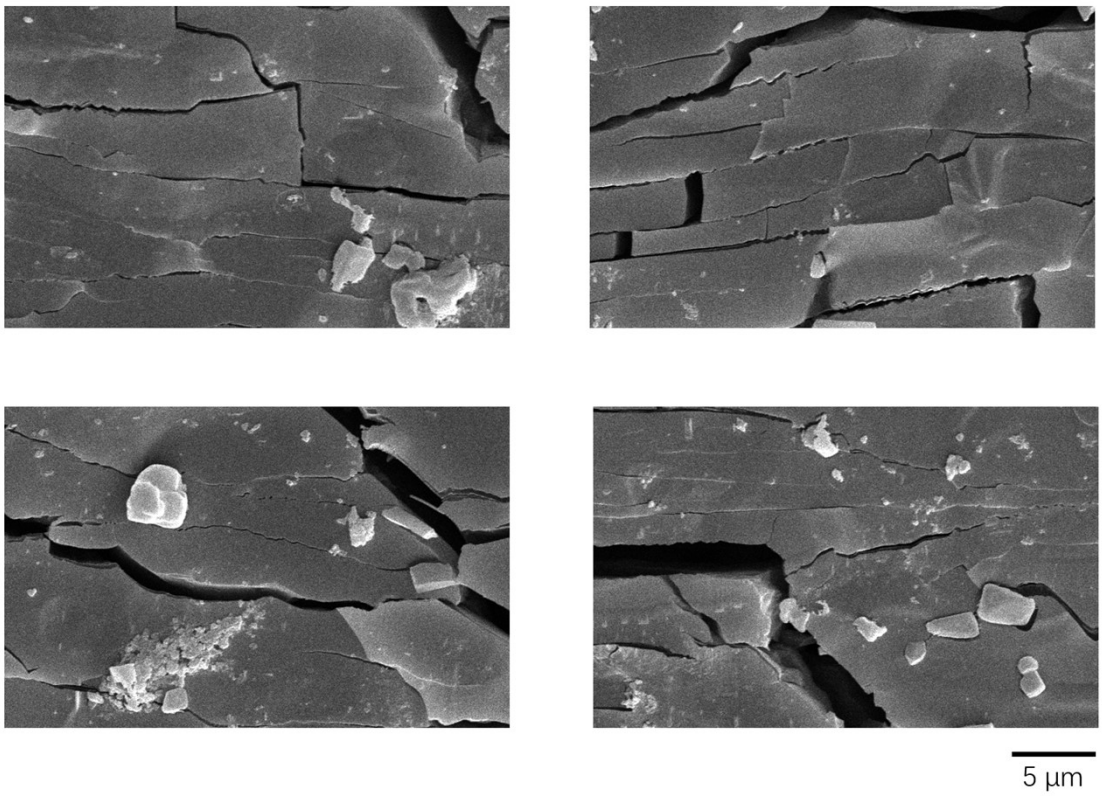

Fig. S18 SEM image of coarse area of **3** at room temperature.

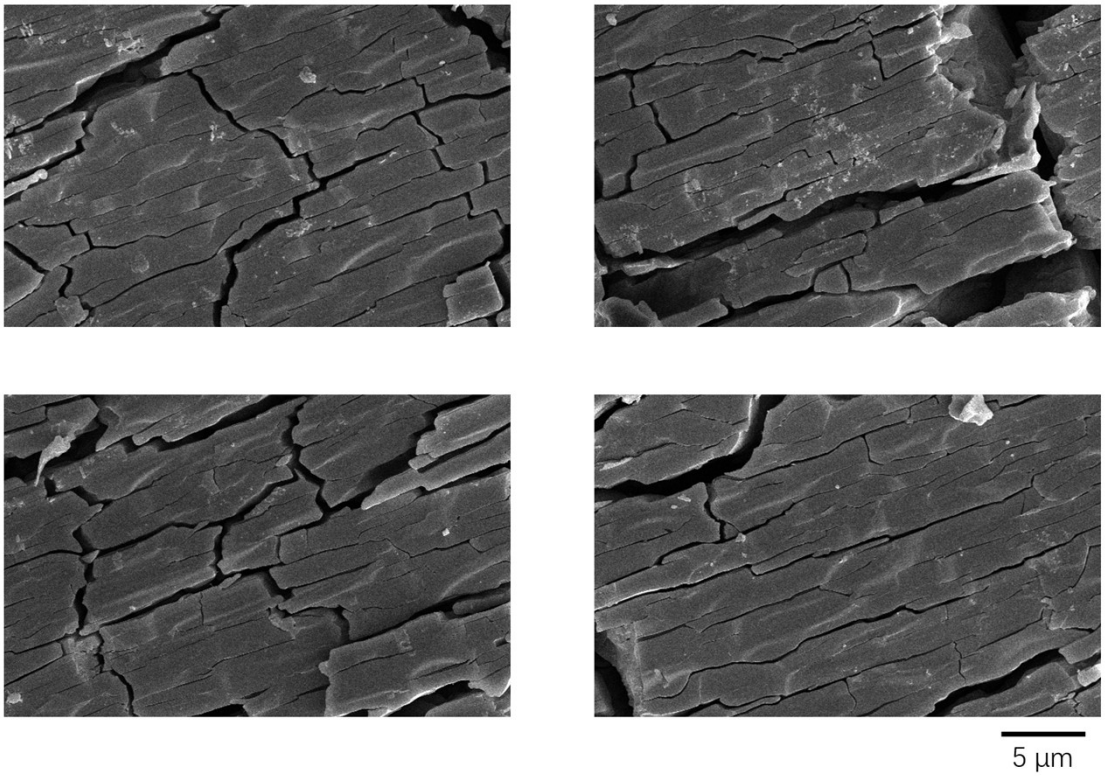

Fig. S19 SEM image of smooth area of **4** at room temperature.

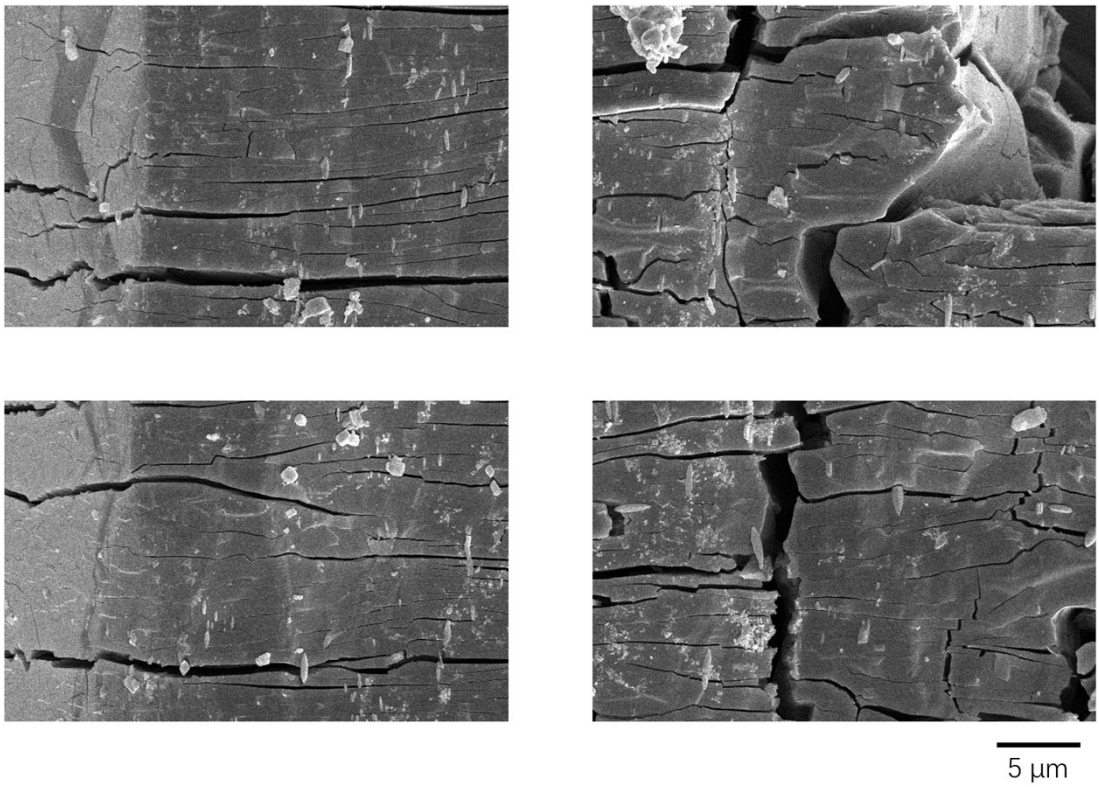

Fig. S20 SEM image of coarse area of **1** at room temperature.

Tab. S1 Crystal structure of **1, 2, 3** at different temperature.

	1	**2**	**2**	**3**	**3**
CCDC number	2248824	2248825	2268348	2268343	2268345
Empirical formula	$C_{13}H_{20}FeKN_8O$	$C_{13}H_{20}CoKN_8O$	$C_{13}H_{20}CoKN_8O$	$C_{13}H_{18}FeKN_8$	$C_{13}H_{18}FeKN_8$
Formula weight	399.32	402.40	402.40	381.30	381.30
Temperature [K]	150.00	150.0	323.0	323.00	100.00
Crystal system	orthorhombic	orthorhombic	orthorhombic	orthorhombic	orthorhombic
Space group (number)	$P2_12_12_1$ (19)	$P2_12_12_1$ (19)	$Pnma$ (62)	$Cmcm$ (63)	$Pnma$ (62)
a [Å]	8.4554(3)	8.4267(11)	13.734(4)	8.9462(11)	16.2028(8)
b [Å]	13.6020(5)	13.5866(16)	8.566(2)	16.1267(19)	12.4169(8)
c [Å]	16.3290(6)	16.2650(18)	16.278(4)	12.3909(15)	8.7273(5)
α [°]	90	90	90	90	90
β [°]	90	90	90	90	90
γ [°]	90	90	90	90	90
Volume [Å^3]	1878.00(12)	1862.2(4)	1915.1(8)	1787.7(4)	1755.83(17)
Z	4	4	4	4	4
ρ_{calc} [gcm^{-3}]	1.412	1.435	1.396	1.417	1.442
μ [mm^{-1}]	1.042	1.162	1.130	1.087	1.107
F(000)	828	832	832	788	788
Crystal size [mm]	0.11×0.09×0.06	0.06×0.05×0.04	0.06×0.05×0.04	0.13×0.12×0.1	0.1×0.07×0.06
Crystal colour	clear yellow	clear light colourless	clear light colourless	clear light yellow	clear light yellow
Crystal shape	block	cube	cube	block	block
Radiation	MoK_α (λ=0.71073 Å)	MoK_α (λ=0.71073 Å)	MoK_α (λ=0.71073 Å)	MoK_α (λ=0.71073 Å)	MoK_α (λ=0.71073 Å)
2θ range [°]	3.90 to 52.75 (0.80 Å)	3.91 to 52.74 (0.80 Å)	3.88 to 52.86 (0.80 Å)	5.05 to 52.73 (0.80 Å)	5.03 to 52.81 (0.80 Å)
Index ranges	−9 ≤ h ≤ 10 −17 ≤ k ≤ 17 −17 ≤ l ≤ 20	−10 ≤ h ≤ 10 −16 ≤ k ≤ 16 −20 ≤ l ≤ 19	−13 ≤ h ≤ 17 −10 ≤ k ≤ 10 −20 ≤ l ≤ 19	−11 ≤ h ≤ 10 −17 ≤ k ≤ 20 −15 ≤ l ≤ 14	−20 ≤ h ≤ 18 −10 ≤ k ≤ 15 −7 ≤ l ≤ 10
Reflections collected	14567	17141	8316	3620	8186
Independent reflections	3817 R_{int} = 0.0602 R_{sigma} =	3772 R_{int} = 0.0406 R_{sigma} =	1928 R_{int} = 0.0886 R_{sigma} =	1019 R_{int} = 0.0325 R_{sigma} = 0.0331	1880 R_{int} = 0.0746 R_{sigma} =

	0.0559	0.0327	0.0784		0.0541
Completeness to θ = 25.242°	99.5 %	99.0 %	91.0 %	99.3 %	99.9 %
Data / Restraints / Parameters	3817/0/223	3772/0/223	1928/195/160	1019/220/128	1880/0/164
Goodness-of-fit on F^2	1.088	0.986	1.470	1.090	1.037
Final R indexes [$I \geq 2\sigma(I)$]	R_1 = 0.0402 wR_2 = 0.0862	R_1 = 0.0272 wR_2 = 0.0635	R_1 = 0.1332 wR_2 = 0.3412	R_1 = 0.0676 wR_2 = 0.2036	R_1 = 0.0414 wR_2 = 0.0912
Final R indexes [all data]	R_1 = 0.0532 wR_2 = 0.0953	R_1 = 0.0315 wR_2 = 0.0663	R_1 = 0.1657 wR_2 = 0.3739	R_1 = 0.0929 wR_2 = 0.2341	R_1 = 0.0667 wR_2 = 0.1053
Largest peak/hole [eÅ^{-3}]	0.72/-0.35	0.56/-0.26	2.21/-0.88	0.73/-0.67	0.48/-0.60

Tab. S2 Selected atomic coordinates and U_{eq} [Å^2] for **1** at 150 K.

Atom	*x*	*y*	*z*	U_{eq}
Fe1	-0.01123(8)	0.01586(4)	0.89474(4)	0.01720(18)
K2	0.02431(14)	-0.05068(7)	0.63450(6)	0.0221(3)
N1	-0.0057(6)	0.2799(3)	0.3168(2)	0.0266(9)
N6	-0.2074(6)	-0.0263(4)	0.5157(3)	0.0323(11)
N7	0.2794(6)	-0.0786(4)	0.5307(3)	0.0340(12)
N3	-0.2446(6)	-0.0388(4)	0.7552(3)	0.0268(11)
C11	0.1624(6)	-0.0025(4)	0.8188(3)	0.0192(11)
C8	-0.1577(6)	-0.0187(4)	0.8072(3)	0.0211(11)
N4	0.2634(5)	-0.0142(4)	0.7733(3)	0.0267(11)
C9	-0.1884(6)	0.0230(4)	0.9714(3)	0.0255(12)
C10	0.1337(6)	0.0536(4)	0.9808(3)	0.0231(12)
N2	-0.0351(5)	0.2623(3)	0.1706(2)	0.0187(9)
C13	-0.0272(6)	0.1541(3)	0.8643(3)	0.0218(10)
C12	0.0195(8)	-0.1208(3)	0.9220(3)	0.0295(12)
C5	-0.1267(7)	0.2810(4)	0.2474(3)	0.0256(13)
H5A	-0.207203	0.229064	0.255751	0.031

Tab. S3 Selected atomic coordinates and U_{eq} [Å^2] for **2** at 150 K.

Atom	*x*	*y*	*z*	U_{eq}
Co01	0.51175(5)	0.48397(3)	0.60587(2)	0.02152(12)
K02	0.47569(9)	0.55157(5)	0.86655(4)	0.02633(17)
N003	0.9645(3)	0.76098(19)	0.82923(17)	0.0241(6)
N6	0.7419(4)	0.5378(2)	0.74384(19)	0.0309(7)
N4	0.9923(4)	0.77912(19)	0.68209(16)	0.0316(6)
N10	0.7905(4)	0.4734(3)	0.48623(19)	0.0338(7)
N5	0.5304(3)	0.2667(2)	0.65523(19)	0.0335(7)
O008	0.4416(4)	0.3564(2)	0.8377(2)	0.0531(8)
H00S	0.493905	0.322799	0.874825	0.080
H00T	0.488145	0.341230	0.791333	0.080
C009	0.3402(4)	0.5007(3)	0.6801(2)	0.0242(7)
N8	0.2812(4)	0.4233(2)	0.4704(2)	0.0363(7)
C00B	0.5278(4)	0.3483(2)	0.63528(19)	0.0253(7)
C00C	0.3689(4)	0.4477(3)	0.5209(2)	0.0267(7)
C00D	0.8713(4)	0.7801(3)	0.7524(2)	0.0294(8)
H00A	0.817398	0.844727	0.755508	0.035
H00B	0.790288	0.728284	0.744119	0.035
N9	0.4612(5)	0.6999(2)	0.56467(19)	0.0473(10)
N7	0.2381(4)	0.5126(2)	0.72613(19)	0.0307(7)
C00G	1.0187(5)	0.8549(2)	0.8698(2)	0.0333(8)
H00C	1.073851	0.896029	0.829374	0.050
H00D	1.091079	0.839166	0.915077	0.050
H00E	0.926437	0.890465	0.891231	0.050

Tab. S4 Selected atomic coordinates and U_{eq} [Å^2] for **2** at 323 K.

Atom	*x*	*y*	*z*	U_{eq}
Co01	0.76868(11)	1.750000	0.60966(9)	0.0391(6)
K1	0.6937(2)	1.750000	0.87242(16)	0.0514(8)
C003	0.9048(9)	1.750000	0.6351(9)	0.068(3)
C10	0.6342(11)	1.750000	0.5835(11)	0.118(5)
N1	0.9905(10)	1.266(2)	0.6860(8)	0.126(3)
N8	0.7298(5)	1.9945(12)	0.7413(5)	0.0604(17)
N7	0.9854(7)	1.750000	0.6507(8)	0.068(3)
C008	0.7434(6)	1.9039(14)	0.6907(7)	0.0596(17)
C009	0.7910(10)	1.5991(14)	0.5298(7)	0.084(2)
N2	0.9716(9)	1.276(2)	0.8200(9)	0.126(3)
N6	0.8009(8)	1.4949(12)	0.4802(6)	0.084(2)
C4	0.9066(11)	1.246(5)	0.6432(11)	0.127(3)
H4A	0.884962	1.345797	0.622838	0.190
H4B	0.917738	1.177047	0.597861	0.190
H4C	0.857648	1.203136	0.678582	0.190

C7	0.9757(16)	1.124(2)	0.7962(12)	0.127(3)
H7A	0.910876	1.079916	0.792420	0.152
H7B	1.013670	1.063076	0.834815	0.152
N9	0.5547(9)	1.750000	0.5680(9)	0.119(5)
C2	0.8894(13)	1.304(3)	0.8624(13)	0.127(3)

Tab. S5 Selected atomic coordinates and U_{eq} [Å^2] for **3** at 323 K.

Atom	***x***	***y***	***z***	U_{eq}
Fe1	0.500000	0.63474(7)	0.750000	0.0398(5)
K1	1.000000	0.86562(11)	0.750000	0.0515(7)
N1	0.7565(8)	0.7606(4)	0.750000	0.086(3)
N2	0.500000	0.6357(5)	1.0005(5)	0.088(4)
N3	0.2641(8)	0.4962(3)	0.750000	0.0579(17)
C1	0.6582(9)	0.7158(4)	0.750000	0.0541(17)
C2	0.500000	0.6352(4)	0.9085(6)	0.0534(17)
C3	0.3506(8)	0.5491(4)	0.750000	0.0450(15)
N4	-0.008(2)	0.5677(9)	0.4949(12)	0.069(4)
N5	-0.0208(18)	0.4223(8)	0.4967(11)	0.053(3)
C4	0.003(4)	0.6114(11)	0.3968(13)	0.088(5)
H4A	-0.095014	0.620042	0.367826	0.132
H4B	0.062066	0.580302	0.346136	0.132
H4C	0.050006	0.664032	0.409836	0.132
C5	-0.064(3)	0.6229(15)	0.5723(19)	0.112(9)
H5A	-0.000220	0.670677	0.576873	0.169
H5B	-0.066430	0.595318	0.640923	0.169
H5C	-0.163070	0.639927	0.552783	0.169
C6	-0.1035(17)	0.4978(10)	0.4839(18)	0.063(4)

Tab. S6 Selected atomic coordinates and U_{eq} [Å^2] for **3** at 100 K.

Atom	***x***	***y***	***z***	U_{eq}
Fe01	0.63495(3)	0.750000	0.51932(6)	0.01808(19)
K002	0.87069(4)	0.750000	1.02002(9)	0.0218(2)
N003	0.75640(19)	0.750000	0.7917(4)	0.0266(8)
N004	0.49007(18)	0.750000	0.7480(4)	0.0251(8)
N005	0.50697(19)	0.750000	0.2589(4)	0.0299(9)
N006	0.63338(15)	1.0009(2)	0.5257(3)	0.0333(7)
N00E	0.7724(2)	0.750000	0.2750(4)	0.0504(12)
C008	0.5554(2)	0.750000	0.3544(4)	0.0216(9)
C009	0.5449(2)	0.750000	0.6638(4)	0.0187(8)
C00A	0.7123(2)	0.750000	0.6882(4)	0.0196(9)
C00B	0.63413(15)	0.9081(3)	0.5223(3)	0.0244(7)
C00C	0.7225(2)	0.750000	0.3684(4)	0.0284(10)

N1	0.5637(9)	0.4980(17)	0.010(2)	0.018(2)
N007	0.4138(8)	0.5010(18)	-0.031(2)	0.020(3)
C1	0.5165(11)	0.5083(16)	0.1618(13)	0.027(3)
H1A	0.507961	0.436686	0.209226	0.032
H1B	0.546858	0.554714	0.234820	0.032
C2	0.6187(12)	0.596(2)	-0.013(2)	0.033(6)
H2A	0.643270	0.593612	-0.115393	0.049
H2B	0.662538	0.596202	0.064417	0.049

A similar step response of dielectric exhibited by cyano-bridged coordination polymers was shown in **Tab. S7**.

Tab. S7 The Values of the T_c, $\Delta\varepsilon'$ *and* ε'(1 MHz) for selected cyano-bridged coordination polymers.

Material	T_c (K)	ε'**(LT)**	ε'**(HT)**	$\Delta\varepsilon'$	**Ref**
$[(CH_3)_4N]_2[KFe(CN)_6]$	245/253	13.5	16	2.5	4
$(azetidinium)_2[KCr(CN)_6]$	171/174	3	25	22	5
$(azetidinium)_2[KFe(CN)_6]$	186/188	3	35	32	5
$[C(NH_2)_3]_2[KFe(CN)_6]$	406/411 435/439	- -	- -		6
$[CH_3C(NH_2)_2]_2[KFe(CN)_6$	199/201 381/385	4 -	8 -	4 -	6
$[(CH_3)NH_3]_2[KFe(CN)_6]$	429/423	5.3	20	15	7
$[(CH_3)_2NH_2]_2[KFe(CN)_6]$	226/224	5.1	18	12.9	7
$[(CH_3)_3NH_1]_2[KFe(CN)_6]$	316/312	5.5	7.1	1.6	7
$[(CH_3)_4N]_2[KFe(CN)_6]$	350/348	4.5	4.5	-	7
$(HIm)_2[KFe(CN)_6]$	158	7.5	23	15.5	8
$(C_7N_2H_{18})[KFe(CN)_6]$	153	6.8	8.1	1.3	**This work**
$(C_7N_2H_{18})[KFe(CN)_6]$	159	6.3	7.1	0.8	**This work**

Reference

1. J. Zhang and T. Lu, Efficient evaluation of electrostatic potential with computerized optimized code, *Phys. Chem. Chem. Phys.*, 2021, **23**, 20323-20328.
2. T. Lu and F. Chen, Quantitative analysis of molecular surface based on improved Marching Tetrahedra algorithm, *J. Mol. Graphics Modell.*, 2012, **38**, 314-323.
3. D. Jayatilaka, S. K. Wolff, D. J. Grimwood, J. J. McKinnon and M. A. Spackman, CrystalExplorer: a tool for displaying Hirshfeld surfaces and visualising intermolecular interactions in molecular crystals, *Acta Crystallogr.*, Sect. A: Found. Adv., 2006, **62**, S90-S90.
4. X.-G. Chen, Z.-X. Zhang, Y.-L. Zeng, S.-Y. Tang and R.-G. Xiong, H/F Substitution induced switchable coordination bonds in a cyano-bridged hybrid double perovskite ferroelastic, *Chem. Commun.*, 2022, **58**, 3059-3062.
5. M. Rok, M. Moskwa, J. Hetmańczyk, Ł. Hetmańczyk and G. Bator, Switchable dielectric constant, structural and vibrational studies of double perovskite organic–inorganic hybrids: (azetidinium)$_2$[KCr(CN)$_6$] and (azetidinium)$_2$[KFe(CN)$_6$], *Crystengcomm*, 2022, **24**, 4932-4939.
6. W.-J. Xu, K.-P. Xie, Z.-F. Xiao, W.-X. Zhang and X.-M. Chen, Controlling Two-Step Phase Transitions and Dielectric Responses by A-Site Cations in Two Perovskite-like Coordination Polymers, *Cryst. Growth Des.*, 2016, **16**, 7212-7217.
7. W.-J. Xu, S.-L. Chen, Z.-T. Hu, R.-B. Lin, Y.-J. Su, W.-X. Zhang and X.-M. Chen, The cation-dependent structural phase transition and dielectric response in a family of cyano-bridged perovskite-like coordination polymers, *Dalton Trans.*, 2016, **45**, 4224-4229.
8. W. Zhang, Y. Cai, R.-G. Xiong, H. Yoshikawa and K. Awaga, Exceptional Dielectric Phase Transitions in a Perovskite-Type Cage Compound, *Angew. Chem., Int. Ed.*, 2010, **49**, 6608-6610.